$CD4^+$ T cells. HHV-6 infection of $CD4^+$ T cells is an indispensable event for the virus replication and reactivation (21). Our *in vitro* experiments suggest that the monomyeloid precursors lead to this critical event in $CD4^+$ T cells and that HHV-6 infects $CD4^+$ T cells in DIHS skin. Furthermore, our results suggest that HMGB-1 released from damaged DIHS skin may be a cue signal for HHV-6 reactivation. Our observations will provide new perspectives toward understanding the pathology of severe drug hypersensitivity bridging over allergy and viral infection, which remains poorly understood, in DIHS.

Acknowledgments

We thank Keiko Sugaya and Makoto Itoi for technical support. This study was supported in part by a Grant-in-Aid for Scientific Research (No. 21591458) and a Health and Labor Sciences Research Grant (Research on Intractable Diseases) from the Ministry of Health, Labour and Welfare of Japan (H24-nanchi-ippan-003).

Authors' contributions

HH had full access to all the data in this study and takes responsibility for the integrity of the data and the accuracy of the data analyses. HH involved in study concept and design; HH, TF, JK, YK, MH, and HY contributed to acquisition of data; HH, TF, and JK analyzed and interpreted the data; HH drafted the manuscript; TF contributed to critical revision of the manuscript for important intellectual content; HH obtained funding; HH, TF, JK, YK, MH, and HY provided administrative, technical, and material support; TF and HY involved in study supervision.

Conflict of interest

The authors have declared that they have no conflicts of interest.

Supporting Information

Additional Supporting Information may be found in the online version of this article:

Figure S1. Phenotypic analysis of the cells in the R1 and R2 population in Figure 1A.

Figure S2. Expression of HHV-6 Ag in CD14+ PBMCs and the monocyte/monomyeloid precursor-rich fractions from a healthy individual and a DIHS patient.

Figure S3. CD11b+(red) CD13+(green) cells residing in the epidermis of some sections of AGEP skin.

Figure S4. Relative HMGB-1 mRNA expression of SJS/TEN skin (n = 3) and DIHS skin (n = 3).

References

1. Shiohara T, Inaoka M, Kano Y. Drug-induced hypersensitivity syndrome (DIHS): a reaction induced by a complex interplay among herpesviruses and antiviral and antidrug immune responses. *Allergol Int* 2006;**55**:1–8.
2. Hashimoto K, Yasukawa M, Tohyama M. Human herpesvirus 6 and drug allergy. *Curr Opin Allergy Clin Immunol* 2003;**3**: 255–260.
3. Shiohara T, Kano Y. A complex interaction between drug allergy and viral infection. *Clin Rev Allergy Immunol* 2007;**33**:124–133.
4. Tohyama M, Hashimoto K, Yasukawa M, Kimura H, Horikawa T, Nakajima K et al. Association of human herpesvirus 6 reactivation with the flaring and severity of drug-induced hypersensitivity syndrome. *Br J Dermatol* 2007;**157**:934–940.
5. Hashizume H, Hansen A, Poulsen LK, Thomsen AR, Takigawa M, Thestrup-Pedersen K. In vitro propagation and dynamics of T cells from skin biopsies by methods using interleukins-2 and -4 or anti-CD3/CD28 antibody-coated microbeads. *Acta Derm Venereol* 2010;**90**:463–473.
6. Elliott MJ, Vadas MA, Eglinton JM, Park LS, To LB, Cleland LG et al. Recombinant human interleukin-3 and granulocyte-macrophage colony-stimulating factor show common biological effects and binding characteristics on human monocytes. *Blood* 1989;**74**:2349–2359.
7. Pozo F, Tenorio A. Detection and typing of lymphotropic herpesviruses by multiplex polymerase chain reaction. *J Virol Methods* 1999;**79**:9–19.
8. Hashizume H, Takigawa M, Tokura Y. Characterization of drug-specific T cells in phenobarbital-induced eruption. *J Immunol* 2002;**168**:5359–5368.
9. Hashizume H, Seo N, Ito T, Takigawa M, Yagi H. Promiscuous interaction between gold-specific T cells and APCs in gold allergy. *J Immunol* 2008;**181**:8096–8102.
10. Hashizume H, Aoshima M, Ito T, Seo N, Takigawa M, Yagi H. Emergence of circulating monomyeloid precursors predicts reactivation of human herpesvirus-6 in drug-induced hypersensitivity syndrome. *Br J Dermatol* 2009;**161**:486–488.
11. van Lochem EG, van der Velden VH, Wind HK, te Marvelde JG, Westerdaal NA, van Dongen JJ. Immunophenotypic differentiation patterns of normal hematopoiesis in human bone marrow: reference patterns for age-related changes and disease-induced shifts. *Cytometry B Clin Cytom* 2004;**60**: 1–13.
12. Mollen KP, Levy RM, Prince JM, Hoffman RA, Scott MJ, Kaczorowski DJ et al. Systemic inflammation and end organ damage following trauma involves functional TLR4 signaling in both bone marrow-derived cells and parenchymal cells. *J Leukoc Biol* 2008;**83**:80–88.
13. Lotze MT, Tracey KJ. High-mobility group box 1 protein (HMGB1): nuclear weapon in the immune arsenal. *Nat Rev Immunol* 2005;**5**:331–342.
14. Bianchi ME, Manfredi AA. High-mobility group box 1 (HMGB1) protein at the crossroads between innate and adaptive immunity. *Immunol Rev* 2007;**220**:35–46.
15. Palumbo R, Galvez BG, Pusterla T, De Marchis F, Cossu G, Marcu KB et al. Cells migrating to sites of tissue damage in response to the danger signal HMGB1 require NF-kappaB activation. *J Cell Biol* 2007;**179**:33–40.
16. Klune JR, Dhupar R, Cardinal J, Billiar TR, Tsung A. HMGB1: endogenous danger signaling. *Mol Med* 2008;**14**:476–484.
17. Wang H, Bloom O, Zhang M, Vishnubhakat JM, Ombrellino M, Che J et al. HMG-1 as a late mediator of endotoxin lethality in mice. *Science* 1999;**285**:248–251.
18. Nakajima S, Watanabe H, Tohyama M, Sugita K, Iijima M, Hashimoto K et al. High-mobility group box 1 protein (HMGB1) as a novel diagnostic tool for toxic epidermal necrolysis and Stevens-Johnson syndrome. *Arch Dermatol* 2011;**147**:1110–1112.

19. Popovic K, Ek M, Espinosa A, Padyukov L, Harris HE, Wahren-Herlenius M et al. Increased expression of the novel proinflammatory cytokine high mobility group box chromosomal protein 1 in skin lesions of patients with lupus erythematosus. *Arthritis Rheum* 2005;**52**:3639–3645.
20. Straino S, Di Carlo A, Mangoni A, De Mori R, Guerra L, Maurelli R et al. High-mobility group box 1 protein in human and murine skin: involvement in wound healing. *J Invest Dermatol* 2008;**128**:1545–1553.
21. Dockrell DH. Human herpesvirus 6: molecular biology and clinical features. *J Med Microbiol* 2003;**52**(Pt 1):5–18.
22. Lusso P, Malnati M, De Maria A, Balotta C, DeRocco SE, Markham PD et al. Productive infection of CD4+ and CD8+ mature human T cell populations and clones by human herpesvirus 6. Transcriptional down-regulation of CD3. *J Immunol* 1991;**147**:685–691.
23. Ancuta P, Liu KY, Misra V, Wacleche VS, Gosselin A, Zhou X et al. Transcriptional profiling reveals developmental relationship and distinct biological functions of CD16+ and CD16- monocyte subsets. *BMC Genomics* 2009;**10**:403.
24. Martinez FO. The transcriptome of human monocyte subsets begins to emerge. *J Biol* 2009;**8**:99.
25. Gordon S, Taylor PR. Monocyte and macrophage heterogeneity. *Nat Rev Immunol* 2005;**5**:953–964.
26. Platzer B, Jorgl A, Taschner S, Hocher B, Strobl H. RelB regulates human dendritic cell subset development by promoting monocyte intermediates. *Blood* 2004;**104**:3655–3663.
27. Kondo K, Kondo T, Okuno T, Takahashi M, Yamanishi K. Latent human herpesvirus 6 infection of human monocytes/macrophages. *J Gen Virol* 1991;**72**(Pt 6):1401–1408.
28. Santangelo S, Gamelli RL, Shankar R. Myeloid commitment shifts toward monocytopoiesis after thermal injury and sepsis. *Ann Surg* 2001;**233**:97–106.
29. Ishida Y, Gao JL, Murphy PM. Chemokine receptor CX3CR1 mediates skin wound healing by promoting macrophage and fibroblast accumulation and function. *J Immunol* 2008;**180**:569–579.
30. Livingston DH, Anjaria D, Wu J, Hauser CJ, Chang V, Deitch EA et al. Bone marrow failure following severe injury in humans. *Ann Surg* 2003;**238**:748–753.
31. Kitamura K, Asada H, Iida H, Fukumoto T, Kobayashi N, Niizeki H et al. Relationship among human herpesvirus 6 reactivation, serum interleukin 10 levels, and rash/graft-versus-host disease after allogeneic stem cell transplantation. *J Am Acad Dermatol* 2008;**58**:802–809.
32. Bellon T, Alvarez L, Mayorga C, Morel E, Torres MJ, Martin-Diaz MA et al. Differential gene expression in drug hypersensitivity reactions: induction of alarmins in severe bullous diseases. *Br J Dermatol* 2010;**162**:1014–1022.
33. Tagami K, Yujiri T, Tanimura A, Mitani N, Nakamura Y, Ariyoshi K et al. Elevation of serum high-mobility group box 1 protein during granulocyte colony-stimulating factor-induced peripheral blood stem cell mobilisation. *Br J Haematol* 2006;**135**:567–569.

Stevens-Johnson syndrome/toxic epidermal necrolysis mouse model generated by using PBMCs and the skin of patients

Nao Saito, MD,[a]* Naoya Yoshioka, PhD,[a]* Riichiro Abe, MD, PhD,[a] Hongjiang Qiao, MD, PhD,[a] Yasuyuki Fujita, MD, PhD,[a] Daichi Hoshina, MD,[a] Asuka Suto, DVM,[a] Satoru Kase, MD, PhD,[b] Nobuyoshi Kitaichi, MD, PhD,[b] Michitaka Ozaki, MD, PhD,[c] and Hiroshi Shimizu, MD, PhD[a] *Sapporo, Japan*

Background: Stevens-Johnson syndrome (SJS) and toxic epidermal necrolysis (TEN) are life-threatening cutaneous reactions caused by drugs or infections and exhibiting widespread epidermal necrosis. Currently, there is no animal model that reproduces SJS/TEN symptoms.
Objective: We sought to develop a novel mouse model of SJS/TEN by using PBMCs and skin from patients who had recovered from SJS/TEN.
Methods: For our mouse model, patients' PBMCs were injected intravenously into immunocompromised NOD/Shi-*scid*, IL-2Rγ^{null} (NOG) mice, followed by oral administration of a causative drug. Subsequently, to replace human skin, unaffected skin specimens obtained from patients who had recovered from SJS/TEN were grafted onto NOG mice, after which patient-derived PBMCs and the causative drug were applied.
Results: Mice injected with PBMCs from patients with SJS/TEN and given the causative drug showed marked conjunctival congestion and numerous cell death of conjunctival epithelium, whereas there were no symptoms in mice injected with PBMCs from patients with ordinary drug skin reactions. $CD8^+$ T lymphocyte–depleted PBMCs from patients with SJS/TEN did not elicit these symptoms. In addition, skin-grafted mice showed darkening of the skin-grafted areas. Cleaved caspase-3 staining showed that dead keratinocytes were more numerous in the skin-grafted mice than in the healthy control animals.
Conclusion: We have established a novel human-oriented SJS/TEN mouse model and proved the importance of $CD8^+$ T lymphocytes in SJS/TEN pathogenesis. The mouse model promises to promote diagnostic and therapeutic approaches.
(J Allergy Clin Immunol 2013;131:434-41.)

Key words: *Stevens-Johnson syndrome, toxic epidermal necrolysis, animal models*

Abbreviations used
APC: Antigen-presenting cell
CTL: Cytolytic T lymphocyte
DC: Dendritic cell
FITC: Fluorescein isothiocyanate
GVHD: Graft-versus-host disease
GVHR: Graft-versus-host reaction
NK: Natural killer
NOG: NOD/Shi-*scid*, IL-2Rγ^{null}
ODSR: Ordinary drug skin reaction
PE: Phycoerythrin
sFasL: Soluble Fas ligand
SJS: Stevens-Johnson syndrome
TEN: Toxic epidermal necrolysis
TUNEL: Terminal deoxynucleotidyl transferase–mediated dUTP nick end labeling

Stevens-Johnson syndrome (SJS) and toxic epidermal necrolysis (TEN) are rare, life-threatening mucocutaneous reactions characterized by extensive detachment of the epidermis.[1] They are considered part of the same spectrum of diseases but with different severities. Patients with SJS have skin detachment on less than 10% of the body surface area, whereas patients with TEN have more extensive lesions.[2] The overall incidences of SJS and TEN have been estimated at 1 to 6 cases per million person-years and 0.4 to 1.2 cases per million person-years, respectively. The mortality associated with TEN is 25%. The eruptions are initially distributed on the face, trunk, and extremities but can rapidly extend to the whole body within just a few hours. Mucous membrane involvement is observed in approximately 90% of cases. Approximately 85% of patients have conjunctival lesions. Ocular complications include chronic conjunctivitis, conjunctival scarring, corneal vascularization, and corneal damage, which can lead to blindness. Ocular morbidity and visual loss can be caused by acute corneal complications, and progressive conjunctival scarring is also significantly associated with subsequent loss of vision.[3] Several treatments have been attempted, including high-dose corticosteroids, intravenous immunoglobulin, and plasmapheresis; however, some cases are resistant to these therapies.[4] In some cases only supportive therapy is applied out of concern over the immunosuppressive effect of these treatments.[5]

The pathologic mechanisms of SJS/TEN are not fully known.[6] Several mediators to induce SJS/TEN have been proposed, such as Fas ligand,[7] soluble Fas ligand (sFasL),[8] perforin, granzyme B,[9] and granulysin.[10,11] These mechanisms can induce massive epithelial cell death. Nevertheless, no one has been able to explain why these systemic "cell-death mediators" affect skin

From the Departments of [a]Dermatology, [b]Ophthalmology, and [c]Molecular Surgery, Hokkaido University Graduate School of Medicine.
*These authors contributed equally to this work.
Supported in part by Health and Labor Sciences Research Grants from the Ministry of Health, Labor, and Welfare of Japan (Research on Allergic Diseases and Immunology; H21-Meneki-Wakate-009 to R.A.) and by the Akiyama Life Science Foundation (to R.A.).
Disclosure of potential conflict of interest: The authors declare that they have no relevant conflicts of interest.
Received for publication February 27, 2012; revised July 28, 2012; accepted for publication September 13, 2012.
Available online October 27, 2012.
Corresponding authors: Riichiro Abe, MD, PhD, Department of Dermatology, Hokkaido University Graduate School of Medicine, N15 W7, Kita-ku, Sapporo 060-8638, Japan. E-mail: aberi@med.hokudai.ac.jp. Or: Hiroshi Shimizu, MD, PhD, Department of Dermatology, Hokkaido University Graduate School of Medicine, N15 W7, Sapporo 060-8638, Japan. E-mail: shimizu@med.hokudai.ac.jp.
0091-6749/$36.00

http://dx.doi.org/10.1016/j.jaci.2012.09.014

exclusively and result in widespread mucocutaneous erosions without dysfunction of other organs. Indeed, serum sFasL levels are increased not only in patients with SJS/TEN but also in those with viral infections[12] and graft-versus-host disease (GVHD).[13]

Because there is only 1 available animal model, basic research on SJS/TEN is still quite preliminary. Azukizawa et al[14,15] generated transgenic mice that express the foreign antigen ovalbumin only on keratinocytes. Injections of ovalbumin-specific cytotoxic T cells induced erosive skin manifestations and numerous apoptotic keratinocytes. Although this model showed widespread erosions and partially elucidated the pathomechanisms of skin lesions in patients with SJS/TEN, the model did not reproduce the drug-specific immune reactions that occur in the patients' blood cells and skin component cells. A more precise drug-triggered SJS/TEN mouse model is urgently required for a more complete understanding of SJS/TEN pathomechanisms and preclinical studies for novel therapeutic strategies.

In light of this, we aimed to develop a relevant animal model of SJS/TEN using patients' tissue samples to reproduce a reaction identical to that of SJS/TEN. Using immunocompromised mice, we successfully evoked the same reactions between the causative drug and human immune cells.

METHODS

Patients' samples

A total of 6 patients with SJS/TEN participated in this study (the patient information is detailed in the Table E1 in this article's Online Repository at www.jacionline.org). The causative drugs were acetaminophen in 4 patients, amoxicillin in 1 patient, and phenytoin in 1 patient. Blood samples were taken from patients with SJS/TEN at least 6 months to 3 years after complete remission of symptoms. Skin biopsy specimens were taken at least 1 year after complete remission of symptoms. The patients had received no systemic glucocorticoids before the study. Ordinary drug skin reactions (ODSRs) in our experiments included the maculopapular type and excluded other adverse drug reactions, such as drug-induced hypersensitivity syndrome/drug rash with eosinophilia and systemic symptoms and acute generalized exanthematous pustulosis. Samples were obtained from Hokkaido University Hospital. The collection of samples was approved by the local ethics committee and the institutional review board of Hokkaido University, and each patient provided written informed consent.

Mice

Immunocompromised NOD/Shi-*scid*, IL-2Rγ^{null} (NOG) mice at 6 to 7 weeks of age were purchased from the Central Institute for Experimental Animals (Tokyo, Japan). With human PBMCs, NOG mice have been used as models of human disease, such as HIV infection.[16] All the animal experiments were performed under the approval of the ethics committee for animal studies of Hokkaido University.

Analysis of graft-versus-host reactions

A graft-versus-host reaction (GVHR) was induced by means of intravenous injection of human PBMCs. Whole PBMCs (1×10^7) were obtained from healthy control subjects, suspended in 0.1 mL of PBS, and then injected intravenously into NOG mice. Skin, ocular, and mucous manifestations were observed. Body weight was monitored. Peripheral blood and splenocytes were analyzed by using flow cytometry to detect human cells. Skin and ocular lesions were investigated histopathologically.

ELISpot IFN-γ assay

PBMCs were prepared from patients' blood and isolated by using Ficoll-Isopaque (Pharmacia Fine Chemicals, Piscataway, NJ) density gradient centrifugation. Mouse peripheral cells and splenocytes were also isolated. The number of IFN-γ–producing cells was determined by using an ELISpot assay kit (Human IFN-γ ELISpot PVDF-Enzymatic; Diaclone, Besancon, France). Ninety-six-well nitrocellulose plates were washed 3 times with PBS before use, and PBMCs (2×10^5 in 100 μL) were incubated overnight with causative drugs in RPMI-1640 medium supplemented with 2 mmol/L L-glutamine, 25 mmol/L HEPES buffer, and 10% heat-inactivated autologous serum. Plates were washed 3 times with PBS, incubated for 2 hours with a biotinylated anti–IFN-γ antibody, and extensively washed. IFN-γ spot-forming cells were developed by using streptavidin–alkaline phosphatase, incubated for 2 hours, and washed before addition of the substrate (5-bromo-4-chloro-3-indolyl-phosphate). The number of spots was counted by using a dissecting microscope (SMZ1500; Nikon, Tokyo, Japan), and the frequency of IFN-γ lymphocytes was defined as the number of spots in 2×10^5 mononuclear cells. The drug-specific reactions between antigen-presenting cells (APCs) and antigen-specific T cells resulted in production of IFN-γ from drug-specific lymphocytes (ie, the IFN-γ–producing T cells are antigen-specific [causative drug–specific] T cells). Using the ELISpot assay, we detected causative drug–specific T cells.

SJS/TEN mouse model using patients' PBMCs

PBMCs were obtained from patients who had recovered from SJS/TEN. In some experiments isolated PBMCs were restimulated with causative drugs in completed RPMI media for 6 days. In other experiments $CD4^+$ or $CD8^+$ cells in PBMCs were depleted by using a magnet-activated cell sorter (MACS; Miltenyi Biotec, Bergisch Gladbach, Germany). PBMCs (2×10^6) were injected intravenously into the NOG mice, followed by oral administration of the causative drugs (acetaminophen, amoxicillin, or phenytoin, 100 μL). The dosage used in the model mice was based on milligrams per kilogram of body weight converted from the adult human normal dose. We administered the drug to the mice once daily. In addition, we confirmed that the dosage was under the median lethal dose in mice. Drug dosage was estimated by dose conversion by body weight. We checked for any changes of the skin, eyes, and mucosa, such as skin color or mucous hemorrhage. Peripheral blood and splenocytes were analyzed by using flow cytometry to detect human cells. Skin, ocular, and liver lesions were investigated by means of histopathologic examination and immunohistochemical staining.

Flow cytometric analysis

Cells were stained with the following antibodies: phycoerythrin (PE)–conjugated mouse CD45, fluorescein isothiocyanate (FITC)–conjugated human CD45, peridinin-chlorophyll-protein complex–conjugated human CD3, FITC-conjugated human CD4, PE-conjugated human CD8, or PE-Cy7–conjugated humanCD56 (BD Biosciences, San Jose, Calif). Analysis was performed by using a FACSAria with BD FACSDiva software (BD Biosciences).

Immunohistochemistry

Immunostaining of ocular, skin, and liver tissues was performed with antibodies to cleaved caspase-3 (Cell Signaling Technology, Beverly, Mass) and human CD4 and CD8 (BD Biosciences). FITC-conjugated goat anti-mouse IgG (Jackson Immunoresearch Laboratories, West Grove, Pa) and TRITC-conjugated rabbit anti-rat IgG (Sigma-Aldrich, St Louis, Mo) were used as secondary antibodies. The nuclei were counterstained with propidium iodide. Fluorescence staining was detected with a confocal laser scanning fluorescence microscope (Fluoview FV1000; Olympus, Tokyo, Japan). We counted the number of stained cells from 5 separate fields, and the average was shown. Terminal deoxynucleotidyl transferase–mediated dUTP nick end labeling (TUNEL) is a method for detecting apoptotic cells with DNA fragmentation by labeling the terminal end of nucleic acids. The TUNEL assay was performed according to the manufacturer's protocol (Takara Bio, Shiga, Japan).

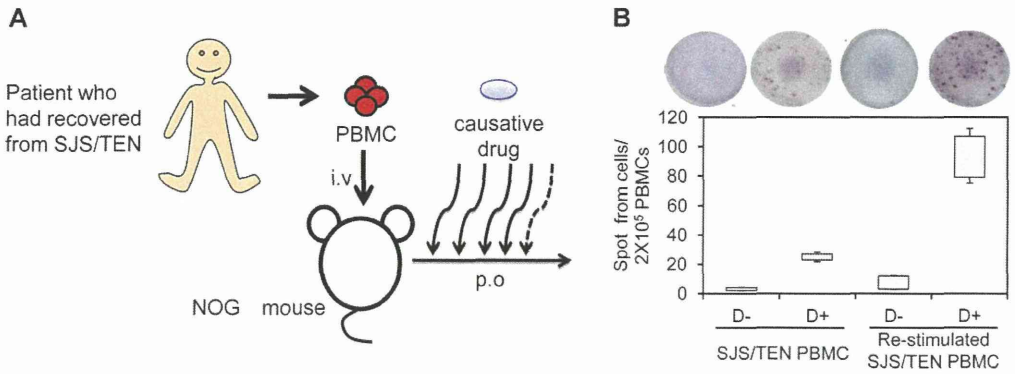

FIG 1. Development of SJS/TEN model mice by using PBMCs of patients who had recovered from SJS/TEN. **A,** Scheme of model mice development. PBMCs were obtained from patients who had recovered from SJS/TEN. These PBMCs (2×10^6) were injected intravenously into NOG mice, followed by oral administration of the causative drugs. **B,** Causative drug–specific cells were detected by using the human IFN-γ ELISpot. When the causative drug was added to cultured PBMCs of patients who had recovered from SJS/TEN (patient 2), causative drug–specific lymphocytes were detected (30 spots per 2×10^5 cells). After 2 stimulations of the causative drug (restimulation), the number of drug-specific lymphocytes increased (90 spots per 2×10^5 cells). Samples from patients 1 to 6 with SJS/TEN were analyzed, and representative data (patient 2) are shown. *i.v.*, Intravenous; *p.o.*, by mouth.

Measurement of human granulysin and human/mouse sFasL

Human granulysin and human/mouse sFasL in supernatants of PBMCs or sera from SJS/TEN model mice were measured by using ELISA. Human granulysin ELISA (BML, Tokyo, Japan) was performed as previously reported.[11] Human/mouse sFasL levels were measured by using an ELISA kit from R&D Systems (Minneapolis, Minn).

SJS/TEN mouse model using patients' PBMCs and skin

Full-thickness skin grafts from healthy control subjects or patients who had recovered from SJS/TEN or an ODSR were transplanted onto the NOG mice. After skin engraftment (approximately 12 days after transplantation), causative drug–stimulated PBMCs (2×10^6) from the same patient were injected intravenously into these mice, followed by oral administration of the causative drug. Changes in skin graft appearance, such as darkening, were observed. The skin grafts were investigated histopathologically.

RESULTS

Development of SJS/TEN mouse model using PBMCs from patients who had recovered from SJS/TEN

To develop the SJS/TEN mouse model, we used PBMCs from patients who had recovered from SJS/TEN. The PBMCs were injected intravenously into immunocompromised mice, followed by oral administration of the causative drug (Fig 1, *A*). There are several reports on the existence of drug-specific lymphocytes in patients who had recovered from drug allergies, and these lymphocytes were restimulated by the causative drug *in vitro*.[17,18] Therefore if lymphocytes that specifically reacted to the drug remained in the peripheral blood, these lymphocytes would be restimulated by the causative drug, and identical immunologic reactions to those of patients with active SJS/TEN would occur in the mice.

First, we confirmed the presence of causative drug–specific lymphocytes in peripheral blood. ELISpot analysis of human IFN-γ was conducted to detect antigen-specific human cells. When the causative drug was added to cultured PBMCs from patients who had recovered from SJS/TEN, causative drug–specific lymphocytes were detected (Fig 1, *B*). After *in vitro* restimulation of the causative drug, the number of drug-specific lymphocytes increased. To exclude the possibility of *in vitro* priming of naive T cells, we performed the ELISpot assay using PBMCs of naive healthy volunteers who had never experienced cutaneous adverse drug reactions. We stimulated the PBMCs of healthy volunteers (n = 4) with amoxicillin, one of the causative drugs in our study, and restimulated them after 5 days. In ELISpot data we were unable to detect drug-specific T cells, even on restimulation (see Fig E1 in this article's Online Repository at www.jacionline.org). Either a breakdown product or a drug metabolite might be the drug form that is responsible for drug reactions that are presumed to be immunologic in nature. On the other hand, in our experiments the addition of native drugs to PBMCs induced the activation of drug-specific lymphocytes, indicating that a breakdown product of the drug might be recognized as an antigen *in vitro*. These data reconfirm that even after resolution of SJS/TEN, drug-specific lymphocytes still circulate, as previously reported.[18]

We used NOG mice, which lack T cells, B cells, and natural killer (NK) cells, as immunocompromised mice.[19] NOG mice are characterized by tolerance to human cells, which enables humanized mice to be established.[20] However, when human cells are applied to NOG mice, GVHRs can occur because engrafted human immune cells attack mouse tissues.[21] The NOG mice showed GVHD symptoms at 46.3 ± 14.3 days after intravenous transplantation of 2.5×10^6 PBMCs.[21] Indeed, at 40 days after human PBMCs were injected intravenously into the NOG mice, weight loss, skin erosion, and diarrhea were noticed as symptoms of GVHRs in our experiments. The skin lesions of patients with GVHRs were quite similar to those of patients with SJS/TEN. Skin erosion and hair loss were observed clinically, and epithelial cell death and epidermal detachment were observed histologically. In addition, human $CD45^+$ cells were detected in mouse peripheral blood at 20 days after PBMC injection (see Fig E2 in this article's Online Repository at www.jacionline.org), showing that activation of injected human cells had occurred in the NOG mice.

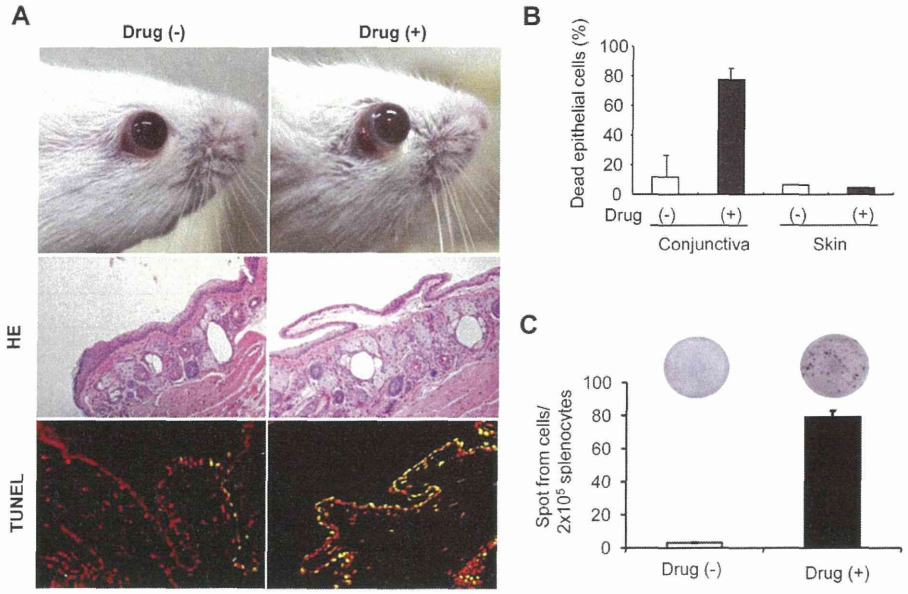

FIG 2. PBMCs from patients with SJS/TEN and causative drug–induced ocular manifestations similar to those of SJS/TEN in NOG mice. **A** and **B,** At 12 days after PBMC injection and causative drug intake, significant conjunctival congestion and conjunctival chemosis are noticed. The PBMC-injected mice without causative drug intake showed no such symptoms. Histologic analysis showed marked edema of the conjunctival subepithelia in the SJS/TEN-PBMC$^+$drug$^+$ mice. The TUNEL assay detected numerous dead epithelial cells in the SJS/TEN-PBMC$^+$drug$^+$ mice (78% of cells) but not in the SJS/TEN-PBMCs$^+$drug$^-$ mice (5% of cells). There was no increase in keratinocyte death in the skin in either group. *HE,* Hematoxylin and eosin. **C,** Human IFN-γ ELISpot with mice splenocytes was performed to confirm that causative drug–specific immune reaction occurred in those mice. At 12 days after PBMC injection, the number of causative drug–specific lymphocytes in the SJS/TEN-PBMC$^+$drug$^+$ mice was significantly increased compared with that of the SJS/TEN-PBMC$^+$drug$^-$ mice. Samples from patients 1, 2, 4, and 5 with SJS/TEN and patient 1 with an ODSR were used, and representative data (patient 2) are shown.

In contrast, within 20 days after PBMC injection, no GVHR symptoms appeared (n = 5). Therefore to distinguish clearly between GVHRs and SJS/TEN reactions, we examined mouse model experiments up to 14 days after PBMC administration.

At 12 days after PBMC injection and causative drug intake, marked conjunctival congestion and conjunctival chemosis were noticed, whereas PBMC-injected mice without causative drug intake showed no such symptoms (Fig 2, *A*). Histologic analysis showed marked edema of the conjunctival subepithelia and vasodilatation in mice receiving PBMCs and causative drug administration (SJS/TEN-PBMC$^+$drug$^+$ mice). We made 20 model mice, all of which showed similar manifestations. Furthermore, the TUNEL assay found numerous dead epithelial cells in the SJS/TEN-PBMC$^+$drug$^+$ mice (78% of cells; Fig 2, *B*) but not in the PBMC-injected, non–drug-administered (SJS/TEN-PBMC$^+$drug$^-$) mice (5% of cells). Unexpectedly, there were no skin manifestations in either group and no difference in percentages of dead keratinocytes between the groups. At 40 days after PBMC injection, weight loss, skin erosion, hair loss, and diarrhea were noticed. Prominent epithelial cell death was observed histologically (see Fig E3 in this article's Online Repository at www.jacionline.org). These data were virtually identical to those of the GVHD model.

To analyze the occurrence mechanism of SJS/TEN in the model mice, we investigated various conditions that might elicit ocular manifestations similar to those of patients with SJS/TEN (Table I). We observed conjunctival congestion and conjunctival chemosis in our model mice.

TABLE I. Occurrence of ocular manifestations in NOG mice in various conditions

Injected cells	*Causative drug intake*	*Ocular manifestations*
PBMCs from patients with SJS/TEN	+	+ (Day 12)
PBMCs from patients with SJS/TEN	−	−
Restimulated PBMCs from patients with SJS/TEN	+	+ (Day 6)
PBMC–depleted CD4$^+$ cells from patients with TEN	+	+ (Day 14)
PBMC–depleted CD4$^+$ cells from patients with TEN	+	−
PBMCs from patients with ODSRs	+	−
PBMCs from patients with ODSRs	−	−
Healthy control PBMCs	+	−
Healthy control PBMCs	−	−
None	+	−

Samples from patients 1 and 2 with SJS/TEN and patient 1 with an ODSR were analyzed, and representative data (patient 2 with SJS/TEN and patient 1 with an ODSR) are shown.

Causative drug intake alone did not induce ocular manifestations in the NOG mice. Healthy control PBMCs and acetaminophen, amoxicillin, or phenytoin, which were the causative drugs in the patients with SJS/TEN described in this article, also did not induce ocular manifestations. Importantly, PBMCs from patients who recovered from ODSRs (ie, nonsevere drug-induced skin reactions) and causative drug intake did not elicit ocular

manifestations. However, we were able to find drug-specific T cells in the spleens of NOG mice after ODSR PBMC transfer and orally administered causative drug by using the same ELISpot assay (see Fig E4 in this article's Online Repository at www.jacionline.org). These data showed the ocular manifestations to be a phenomenon specific to PBMCs from patients with SJS/TEN. In addition, causative drug–restimulated PBMCs from patients with SJS/TEN accelerated the onset of ocular manifestations. $CD4^+$ or $CD8^+$ T lymphocytes were depleted from the PBMCs to identify which lymphocyte subtype is critical in inducing ocular manifestations. $CD4^+$ T lymphocyte–depleted PBMCs from patients with SJS/TEN were able to induce ocular manifestations, whereas $CD8^+$ T lymphocyte–depleted PBMCs from patients with SJS/TEN were not (see Fig E5 in this article's Online Repository at www.jacionline.org).

These data demonstrate that we have succeeded in establishing model mice showing ocular manifestations (ie, SJS/TEN model mice). In addition, the ocular manifestations similar to those of patients with SJS/TEN in NOG mice were found to be dependent on the causative drug–specific lymphocytes of patients with SJS/TEN, and $CD8^+$ T cells are essential to this phenomenon.

Soluble factors, such as granulysin, were not mediators of conjunctival cell death in the SJS/TEN mouse model

In our novel SJS/TEN mouse model, there were almost no infiltrating human cells (human $CD45^+$ cells) in the conjunctiva, whereas numerous human cells were detected in the conjunctiva of the mice with GVHRs (see Fig E6 in this article's Online Repository at www.jacionline.org). Therefore it might be that conjunctival cell death is partially induced by soluble factors in addition to direct lymphocyte-epithelium interaction. As mentioned above, we and others have shown that granulysin might contribute to SJS/TEN occurrence. We examined granulysin levels in the supernatants of causative drug–stimulated PBMCs. Causative drug–stimulated PBMCs from patients with SJS/TEN secreted granulysin at levels less than (0.2 ± 0.3 ng/mL) than the serum levels of patients with acute-phase SJS/TEN (24.8 ± 21.2 ng/mL) and those of healthy control subjects (1.6 ± 0.6 ng/mL).[11] In addition, granulysin immunohistostaining in the conjunctiva of SJS/TEN model mice and in grafted skin from patients with SJS-TEN showed almost no granulysin expression in these tissues (data not shown). Furthermore, human granulysin and sFasL levels in the sera of mice were measured at days 8 and 12. Serum levels of human granulysin and sFasL were undetectable at these time points. Although ELISA for murine granulysin was not available, we measured murine sFasL levels in these samples. We did not detect an increase in murine sFasL levels in sera from SJS/TEN model mice (data not shown). Therefore granulysin was unlikely to be a candidate for mediating conjunctival cell death in SJS/TEN in our model mice.

Development of an SJS/TEN mouse model using PBMCs and the skin of patients who had recovered from SJS/TEN

In our novel SJS/TEN mouse model skin manifestations did not appear; these model mice do not mimic human SJS/TEN completely because the target epithelium was murine in origin. We tried to generate another mouse model to simulate skin manifestations.

First, skin from a patient who had recovered from SJS/TEN was grafted onto the backs of NOG mice. After engraftment was confirmed, PBMCs from the same patient were administered intravenously, followed by oral administration of the causative drug (Fig 3, *A*). In this model both the effector cells and the target cells originate from the same patient with SJS/TEN.

Darkening appeared in the skin graft at 4 days after PBMC injection (Fig 3, *B*). The darkened area increased at 8 days after PBMC injection (Fig 3, *C*). In contrast, we observed no color changes and histologic findings showed few keratinocyte deaths in skin-grafted areas at 8 days after PBMC injection without causative drug intake (see Fig E7 in this article's Online Repository at www.jacionline.org). With PBMCs and skin from the same healthy control subject, no necrotic area appeared. Detection of caspase-3 proves that apoptosis has occurred because it is either partially or totally responsible for the proteolytic cleavage of many key proteins, such as the nuclear enzyme poly (ADPribose) polymerase. Using cleaved caspase-3 staining, we confirmed the increase in keratinocyte death in the SJS/TEN skin graft compared with that seen in the healthy control animals (Fig 3, *D*). In addition, we transplanted skin from patients with ODSRs onto NOG mice and injected the same patients' PBMCs, followed by administration of the causative drug or the vehicle. These mice showed no changes in the appearance of the skin-grafted areas. Histopathologically, the number of apoptotic keratinocytes in ODSR model mice did not differ between the causative drug group and the vehicle group (see Fig E8 in this article's Online Repository at www.jacionline.org).

To investigate the infiltrated cell types, we performed skin graft staining. Both human $CD4^+$ and $CD8^+$ T cells were infiltrated in the transplanted skin areas. However, there were no differences in the numbers of cells between the patient with SJS/TEN and the control (Fig 4). These findings indicate that infiltrating lymphocytes are not critical in this model. The manifestations of these models were quite similar to those in skin lesions of patients with SJS/TEN.

DISCUSSION

The present study aimed to develop a mouse model to mimic human SJS/TEN. We succeeded in reproducing SJS/TEN-like manifestations in the mice. Our results provide an SJS/TEN animal model that promises to be useful in experiments involving SJS/TEN.

To date, investigations to reveal the pathomechanism of SJS/TEN have been carried out with human samples. In previous reports reactions in the acute phase of SJS/TEN in peripheral blood and skin lesions were analyzed, and these investigations have shown that inflammatory mediators, proapoptotic mediators, or infiltrated cells in the skin lesions might be linked to the occurrence of SJS/TEN.

Chung et al[10] attempted to identify key molecules in skin lesions (bullae), and they focused on the most highly expressed proapoptotic molecule: granulysin. Granulysin was found to induce cultured keratinocyte death. Furthermore, recombinant granulysin injection into the murine skin elicited skin necrosis. In addition, we detected higher concentrations of serum granulysin in the acute phase of SJS/TEN than in ODSRs.[11] In contrast,

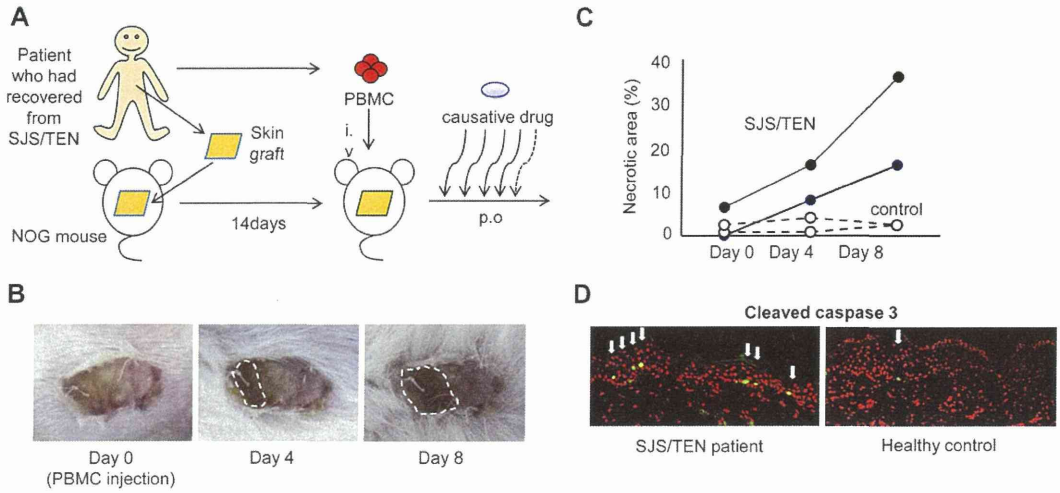

FIG 3. Development of the SJS/TEN mouse model using PBMCs and skin grafts of patients who had recovered from SJS/TEN. **A,** Scheme of mouse model development. Skin grafts from a patient who had recovered from SJS/TEN were grafted onto the backs of NOG mice. After engraftment was confirmed, PBMCs from the same patient were applied intravenously, followed by oral administration of the causative drug. **B** and **C,** Darkened areas appear in the skin graft at 4 days after PBMC injection. These areas were increased at 8 days after PBMC injection. In contrast, the darkened area did not appear in skin grafts of mice when using PBMCs and skin from the healthy control subject. **D,** By using cleaved caspase-3 staining, a great increase in keratinocyte death in the SJS/TEN skin graft was detected in comparison with the keratinocyte death seen in the healthy control specimens. Samples from patient 6 with SJS/TEN and patient 2 with an ODSR were used. *i.v.*, Intravenous; *p.o.*, by mouth.

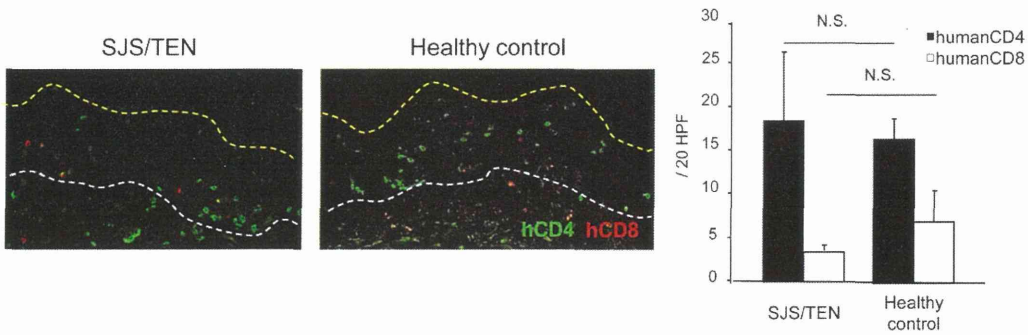

FIG 4. Human CD4 and CD8 staining was performed. Both human $CD4^+$ and $CD8^+$ T cells infiltrated the transplanted skin areas. There were no differences in the numbers of cells between patients with SJS/TEN and controls. Samples from patient 6 with SJS/TEN were used. *HPF,* High-powered field; *N.S.*, not significant.

French's group reported that Fas and Fas ligand interaction is critical in SJS/TEN pathogenesis.[7] They reported that keratinocyte apoptosis in patients with SJS/TEN is mediated by Fas and Fas ligand, which are both expressed on keratinocytes. We also reported that sFasL was able to induce keratinocyte death[8] and that the serum level of sFasL was increased in the acute phase of SJS/TEN, as was the serum level of granulysin.[22] Other candidates, such as α-defensin, have also been reported.[23]

A recent article reported that NK–cytolytic T lymphocyte (CTLs) might be a cell component that contributes to SJS/TEN occurrence. Activated CTLs gain NK cell–like function; these are called NK-CTLs, and they specifically express CD94/NKG2C. NK-CTLs accumulate in skin lesions of patients with SJS/TEN, where they induce keratinocyte death through an interaction between CD94/NKG2C and HLA-E that is expressed specifically on keratinocytes of SJS/TEN lesions.[24]

Even though knowledge regarding the mechanism of SJS/TEN has been accumulated, these findings have never been confirmed in an *in vivo* model. If some molecules were highly expressed in skin lesions or blood during the acute phase of SJS/TEN, there would be no way to confirm whether these molecules are key players. Regarding proapoptotic molecules, several candidates have been reported, as described above. However, most reports focused on molecules that researchers anticipated to contribute to SJS/TEN pathogenesis. Granulysin was identified by means of DNA microarray of cells in bullae; however, not only did the data show that the mRNA level of granulysin was increased, they also showed that the mRNA levels of other proapoptotic molecules, such as Fas ligand, perforin, and granzyme B, were increased.[10] This suggests that several pathways are activated in the apoptotic phenomenon *in vivo*, and there is no solid evidence of an exclusive key player. Animal model experiments involving

depletion or inhibition of specific molecules were essential in proving their uniqueness. Previous experiments with patients' specimens provided fragmentary information on disease etiology. Our model mice open the possibility of recreating the pathologic conditions of SJS/TEN in mice and conducting circumstantial *in vivo* examinations, such as on the benefits of treatments. In our study $CD8^+$ lymphocyte–depleted PBMCs did not produce SJS-like symptoms, strongly demonstrating that $CD8^+$ lymphocytes are necessary to SJS/TEN pathogenesis. Previous reports showed that $CD4^+$ T cells were the predominant population that infiltrated into "maculopapular rash" skin lesions and that most drug-specific T cells were $CD4^+$ T cells.[25] However, in severe cutaneous adverse drug reactions $CD8^+$ T cells were the predominant population that infiltrated into the epidermis of skin lesions of patients with SJS/TEN,[10] and HLA-B*1502 was found to be associated with carbamazepine-induced SJS in all cases.[26] In addition, drug-specific $CD8^+$ T cells were found to predominantly proliferate during the acute stages of SJS.[27] Although drug-specific $CD4^+$ T cells are essential in drug-mediated immune reactions, $CD8^+$ T cells are critical to the development of SJS/TEN. Furthermore, in the skin lesions of model mice, the numbers of $CD4^+$ and $CD8^+$ lymphocytes did not differ between patients with SJS/TEN and control subjects. These findings indicate that infiltrating lymphocytes are not required to generate SJS/TEN skin lesions. Given the findings of ocular lesions, we made the supposition that soluble factors might be involved in keratinocyte death. Although granulysin and sFasL were not specific mediators of this phenomenon, we speculated that causative drug–stimulated PBMCs from patients with SJS/TEN secreted certain cell-death mediators.

Our data using this model also suggest that drug presentation and recognition in the skin might be less necessary than expected because some symptoms develop with little or no recruitment of drug-specific T cells. In our model mice it seems that drug-specific cells were presented and activated by APCs at the spleen and not the skin. Therefore we consider that human APCs presented drug/antigen to T cells in the spleen or peripheral blood. Taken together, we conclude that soluble factors from $CD8^+$ lymphocytes are critical for SJS/TEN development. Our model mice are useful experimental tools to reveal the SJS/TEN pathomechanism.

It is possible that PBMCs from patients with SJS/TEN, which are activated by the causative drug, are highly proliferative and lead to human PBMC reconstitution at day 12, resulting in accelerated GVHRs. However, GVHRs are mediated by human cell infiltration into murine tissue. Indeed, in the GVHR model we detected numerous human cells in the conjunctiva of the mice, whereas in the SJS/TEN-PBMC model, we detected few human cells in conjunctiva and peripheral blood at day 12. These data indicated that at least the ocular manifestations of mice receiving SJS/TEN-PBMC/drug at day 12 were not GVHRs. If PBMCs are highly proliferative at day 12, ocular manifestations can be regarded as a drug-specific phenomenon because mice receiving only PBMCs from patients with SJS/TEN never show such symptoms.

In our model mice it is speculated that the APCs of mice presented drug/antigens to human drug-specific lymphocytes. However the NOG mice used in our experiments have no T, B, and NK cells. In addition, the dendritic cells (DCs) of NOG mice are deficient in antigen presentation.[19] Indeed, dysfunction of DCs allowed engraftment by human cells in NOG mice (ie, DCs of NOG were unable to present xenoantigen to human lymphocytes sufficiently). Therefore we assume that donor human APCs present drug antigens to T cells. Furthermore, by using human IFN-γ ELISpot, the number of drug-specific lymphocytes increased in the spleens of the SJS/TEN-PBMC model mice.

From the clinical aspect, issues have included the difficulty of early diagnosis of SJS/TEN and unresponsiveness to treatment. In the early stage SJS/TEN presents clinically as edematous papules or erythema multiforme–like target rashes that are very similar to those of ODSRs. Such a clinical course makes it difficult to reach a diagnosis of SJS/TEN in the early stage, which results in high mortality rates. Furthermore, the majority of SJS/TEN cases progress rapidly within a few days; therefore methods of early diagnosis are urgently required. We previously analyzed serum samples from 5 patients with SJS/TEN in the early stage (before skin erosions or mucous lesions appeared) and showed that serum levels of sFasL and granulysin are predictors of SJS/TEN diagnosis.[11,22] However, collecting samples at the early stage was quite difficult because of the rarity of the diseases and the intractability of the diagnosis in the early stage, as mentioned above. The present mouse model might allow assessment of changes over time and provide other predictors of early diagnosis and severity of SJS/TEN. Furthermore, treatment interventions are able to be implemented in the early phase in our model, contributing to the prediction of disease onset and prognosis.

We thank Ms Ayumi Moriya for her technical expertise.

Clinical implications: We report a novel mouse model of SJS/TEN that was developed by using PBMCs and skin from patients who had recovered from SJS/TEN. The model promises to promote diagnostic and therapeutic approaches.

REFERENCES

1. Roujeau JC, Kelly JP, Naldi L, Rzany B, Stern RS, Anderson T, et al. Medication use and the risk of Stevens-Johnson syndrome or toxic epidermal necrolysis. N Engl J Med 1995;333:1600-7.
2. Bastuji-Garin S, Rzany B, Stern RS, Shear NH, Naldi L, Roujeau JC. Clinical classification of cases of toxic epidermal necrolysis, Stevens-Johnson syndrome, and erythema multiforme. Arch Dermatol 1993;129:92-6.
3. Di Pascuale MA, Espana EM, Liu DT, Kawakita T, Li W, Gao YY, et al. Correlation of corneal complications with eyelid cicatricial pathologies in patients with Stevens-Johnson syndrome and toxic epidermal necrolysis syndrome. Ophthalmology 2005;112:904-12.
4. Pereira FA, Mudgil AV, Rosmarin DM. Toxic epidermal necrolysis. J Am Acad Dermatol 2007;56:181-200.
5. Schneck J, Fagot JP, Sekula P, Sassolas B, Roujeau JC, Mockenhaupt M. Effects of treatments on the mortality of Stevens-Johnson syndrome and toxic epidermal necrolysis: a retrospective study on patients included in the prospective EuroSCAR Study. J Am Acad Dermatol 2008;58:33-40.
6. Chung WH, Hung SI. Recent advances in the genetics and immunology of Stevens-Johnson syndrome and toxic epidermal necrosis. J Dermatol Sci 2012; 66:190-6.
7. Viard I, Wehrli P, Bullani R, Schneider P, Holler N, Salomon D, et al. Inhibition of toxic epidermal necrolysis by blockade of CD95 with human intravenous immunoglobulin. Science 1998;282:490-3.
8. Abe R, Shimizu T, Shibaki A, Nakamura H, Watanabe H, Shimizu H. Toxic epidermal necrolysis and Stevens-Johnson syndrome are induced by soluble Fas ligand. Am J Pathol 2003;162:1515-20.
9. Posadas SJ, Padial A, Torres MJ, Mayorga C, Leyva L, Sanchez E, et al. Delayed reactions to drugs show levels of perforin, granzyme B, and Fas-L to be related to disease severity. J Allergy Clin Immunol 2002;109:155-61.
10. Chung WH, Hung SI, Yang JY, Su SC, Huang SP, Wei CY, et al. Granulysin is a key mediator for disseminated keratinocyte death in Stevens-Johnson syndrome and toxic epidermal necrolysis. Nat Med 2008;14:1343-50.

11. Abe R, Yoshioka N, Murata J, Fujita Y, Shimizu H. Granulysin as a marker for early diagnosis of the Stevens-Johnson syndrome. Ann Intern Med 2009;151: 514-5.
12. Lee JY, Chae DW, Kim SM, Nam ES, Jang MK, Lee JH, et al. Expression of FasL and perforin/granzyme B mRNA in chronic hepatitis B virus infection. J Viral Hepat 2004;11:130-5.
13. Das H, Imoto S, Murayama T, Kajimoto K, Sugimoto T, Isobe T, et al. Levels of soluble FasL and FasL gene expression during the development of graft-versus-host disease in DLT-treated patients. Br J Haematol 1999;104: 795-800.
14. Azukizawa H, Kosaka H, Sano S, Heath WR, Takahashi I, Gao XH, et al. Induction of T-cell-mediated skin disease specific for antigen transgenically expressed in keratinocytes. Eur J Immunol 2003;33:1879-88.
15. Azukizawa H, Sano S, Kosaka H, Sumikawa Y, Itami S. Prevention of toxic epidermal necrolysis by regulatory T cells. Eur J Immunol 2005;35:1722-30.
16. Nakata H, Maeda K, Miyakawa T, Shibayama S, Matsuo M, Takaoka Y, et al. Potent anti-R5 human immunodeficiency virus type 1 effects of a CCR5 antagonist, AK602/ONO4128/GW873140, in a novel human peripheral blood mononuclear cell nonobese diabetic-SCID, interleukin-2 receptor gamma-chain-knocked-out AIDS mouse model. J Virol 2005;79:2087-96.
17. Beeler A, Engler O, Gerber BO, Pichler WJ. Long-lasting reactivity and high frequency of drug-specific T cells after severe systemic drug hypersensitivity reactions. J Allergy Clin Immunol 2006;117:455-62.
18. Rozieres A, Hennino A, Rodet K, Gutowski MC, Gunera-Saad N, Berard F, et al. Detection and quantification of drug-specific T cells in penicillin allergy. Allergy 2009;64:534-42.
19. Ito M, Hiramatsu H, Kobayashi K, Suzue K, Kawahata M, Hioki K, et al. NOD/SCID/gamma(c)(null) mouse: an excellent recipient mouse model for engraftment of human cells. Blood 2002;100:3175-82.
20. Ito M, Kobayashi K, Nakahata T. NOD/Shi-scid IL2rgamma(null) (NOG) mice more appropriate for humanized mouse models. Curr Top Microbiol Immunol 2008;324:53-76.
21. Ito R, Katano I, Kawai K, Hirata H, Ogura T, Kamisako T, et al. Highly sensitive model for xenogenic GVHD using severe immunodeficient NOG mice. Transplantation 2009;87:1654-8.
22. Murata J, Abe R, Shimizu H. Increased soluble Fas ligand levels in patients with Stevens-Johnson syndrome and toxic epidermal necrolysis preceding skin detachment. J Allergy Clin Immunol 2008;122:992-1000.
23. Morel E, Alvarez L, Cabanas R, Fiandor A, Diaz R, Escamochero S, et al. Expression of alpha-defensin 1-3 in T cells from severe cutaneous drug-induced hypersensitivity reactions. Allergy 2011;66:360-7.
24. Morel E, Escamochero S, Cabanas R, Diaz R, Fiandor A, Bellon T. CD94/NKG2C is a killer effector molecule in patients with Stevens-Johnson syndrome and toxic epidermal necrolysis. J Allergy Clin Immunol 2010;125:703-10, e1-10.
25. Hari Y, Frutig-Schnyder K, Hurni M, Yawalkar N, Zanni MP, Schnyder B, et al. T cell involvement in cutaneous drug eruptions. Clin Exp Allergy 2001;31:1398-408.
26. Chung WH, Hung SI, Hong HS, Hsih MS, Yang LC, Ho HC, et al. Medical genetics: a marker for Stevens-Johnson syndrome. Nature 2004;428:486.
27. Hanafusa T, Azukizawa H, Matsumura S, Katayama I. The predominant drug-specific T-cell population may switch from cytotoxic T cells to regulatory T cells during the course of anticonvulsant-induced hypersensitivity. J Dermatol Sci 2012; 65:213-9.

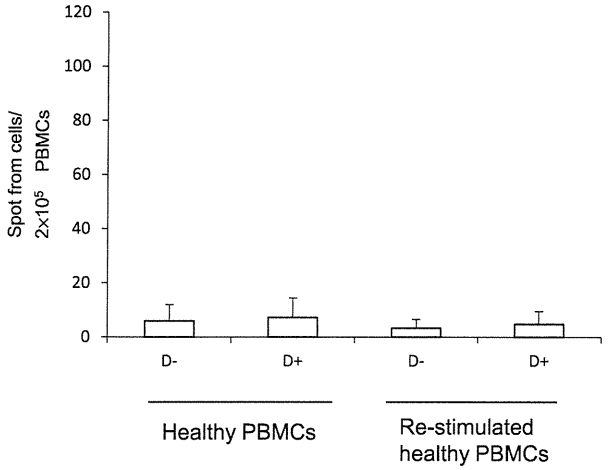

FIG E1. ELISpot assays with PBMCs of naive healthy volunteers who had never experienced cutaneous adverse drug reaction were performed. PBMCs of healthy volunteers (n = 4) were stimulated with amoxicillin, one of the causative drugs in our study, and restimulated after 5 days. ELISpot analysis did not detect drug-specific T cells, even in restimulation. *D+*, Drug addition; *D−*, no drug addition.

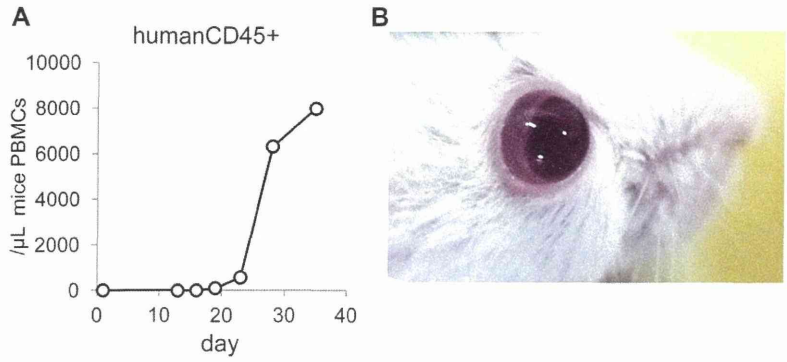

FIG E2. **A,** Human CD45^{+} cells were detected in peripheral blood of NOG mice 20 days after PBMC injection. **B,** Ocular manifestations 14 days after PBMC injection.

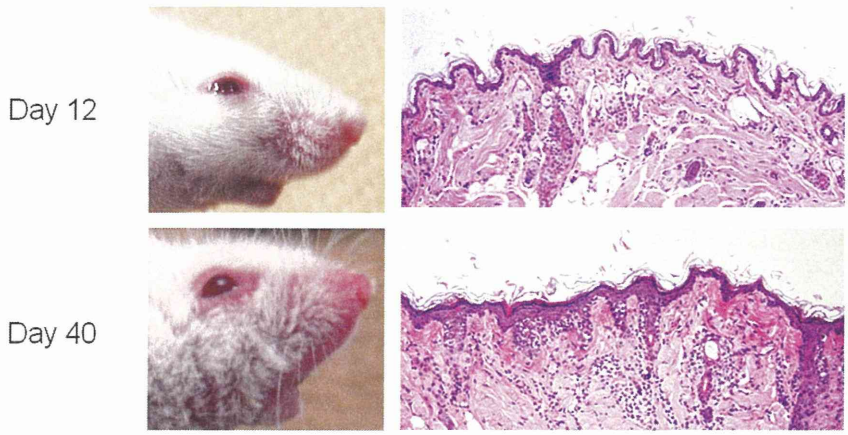

FIG E3. At 12 days after injection of PBMCs from patients with SJS/TEN, NOG mice receiving causative drug showed no significant skin manifestation, and histologic findings indicated intact skin. At 40 days after injection of PBMCs from patients with SJS/TEN, these NOG mice showed weight loss, skin erosion, hair loss, and diarrhea. Prominent epithelial cell death was observed histologically. Samples from patients 1 and 2 with SJS/TEN were analyzed, and representative data (patient 2 with SJS/TEN) are shown.

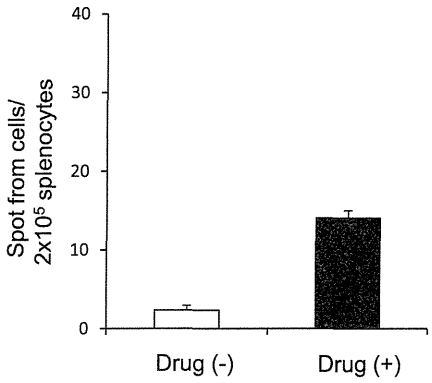

FIG E4. Increase in drug-specific T-cell numbers in the spleens of NOG mice at 12 days after transfer of PBMCs from patients with ODSRs orally given causative drug is detected by using the ELISpot assay. These results are comparable with those for patients with SJS/TEN. Samples from patient 1 with an ODSR were analyzed.

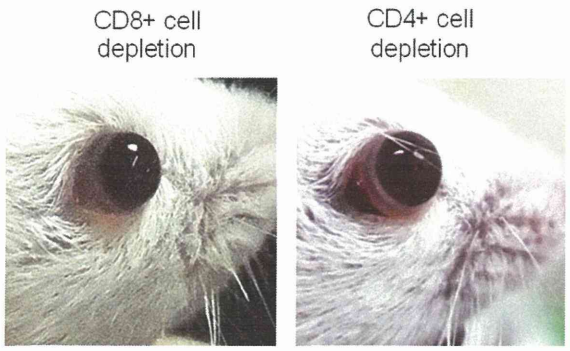

FIG E5. At 12 days after injection of $CD4^+$ T lymphocyte–depleted PBMCs from patients with SJS/TEN and causative drug intake, significant conjunctival congestion and conjunctival chemosis were noticed, whereas this was not the case with $CD8^+$ T lymphocyte–depleted PBMCs from patients with SJS/TEN. Samples from patient 2 with SJS/TEN were analyzed.

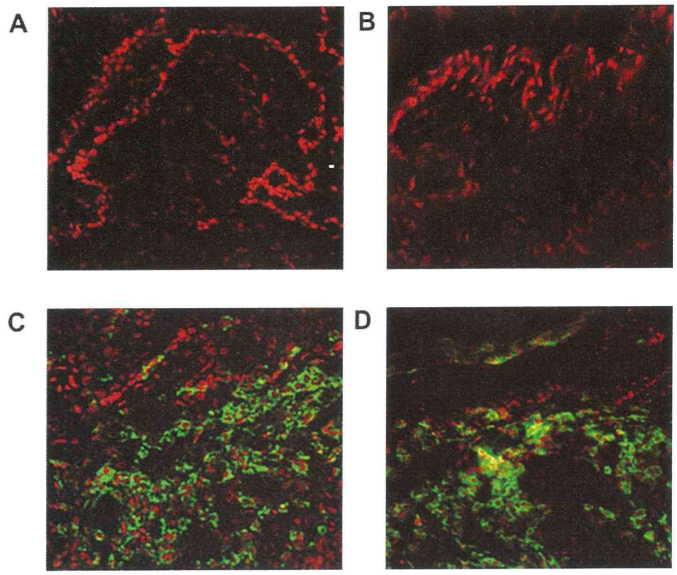

FIG E6. The conjunctiva of SJS/TEN model mice or mice with GVHRs were stained with anti-human CD45 antibodies. FITC-conjugated goat anti-mouse IgG was used as the secondary antibody. The nuclei were counterstained with propidium iodide. **A,** Day 12 for PBMCs from patients with SJS/TEN with causative drug intake. **B,** Day 12 for the GVHD model. **C,** Day 40 for PBMCs from patients with SJS/TEN with causative drug intake. **D,** Day 40 for the GVHD model. In the conjunctiva of both SJS/TEN model and GVHR model mice, there are almost no infiltrating human $CD45^+$ cells at day 12 after PBMC injection, whereas numerous human cells are detected in the conjunctiva of both SJS/TEN model and GVHR model mice. Samples from patients 1 and 2 with SJS/TEN were analyzed, and representative data (patient 2 with SJS/TEN) are shown.

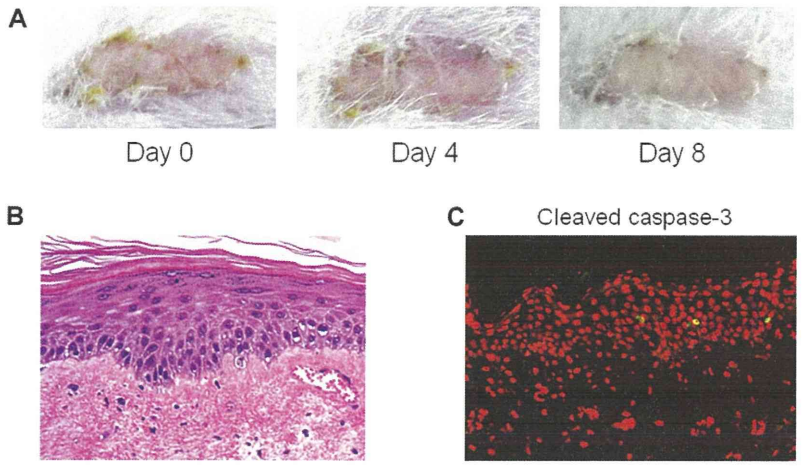

FIG E7. Skin from a patient who had recovered from SJS/TEN was grafted onto the back of NOG mice. After engraftment was confirmed, PBMCs from the same patient were administered intravenously without causative drug administration. Histopathologically, there were few apoptotic keratinocytes in the skin-grafted area. Cleaved caspase-3 staining showed almost no positive cells in the skin-grafted area. Samples from patient 6 with SJS/TEN were analyzed.

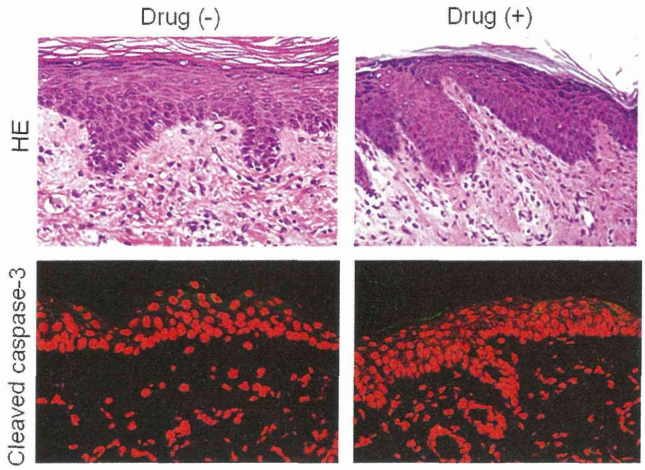

FIG E8. Skin grafts from patients with ODSRs were transplanted onto NOG mice, which were then injected with PBMCs from the same patients, followed by the causative drug or vehicle. These mice showed no changes in appearance of the skin-grafted areas. Histopathologically, there were few dead keratinocytes and few cleaved caspase-3–positive cells in the skin graft. Samples from patient 2 with ODSR were analyzed. *HE*, Hematoxylin and eosin.

TABLE E1. Patient information

Case	Age (y)/sex	Causative drug	Type of cADR	SI
SJS/TEN				
1	55/M	Acetaminophen	TEN	2.4
2	46/M	Acetaminophen	SJS	2.0
3	49/F	Acetaminophen	SJS	2.3
4	49/M	Benzbromarone	SJS	2.9
5	37/F	Amoxicillin	SJS	2.0
6	71/M	Phenytoin	SJS	2.5
ODSR				
1	70/M	Acetaminophen	Maculopapular	2.0
2	78/M	Phenytoin	Maculopapular	6.7

cADR, Cutaneous adverse drug reaction; *F*, female; *M*, male; *SI*, stimulation index.

Visual Improvement after Cultivated Oral Mucosal Epithelial Transplantation

Chie Sotozono, MD, PhD,[1] Tsutomu Inatomi, MD, PhD,[1] Takahiro Nakamura, MD, PhD,[1] Noriko Koizumi, MD, PhD,[1] Norihiko Yokoi, MD, PhD,[1] Mayumi Ueta, MD, PhD,[1] Kotone Matsuyama, BS,[2] Keiko Miyakoda, MS, MPH,[2] Hideaki Kaneda, MD, PhD,[2] Masanori Fukushima, MD, PhD,[2] Shigeru Kinoshita, MD, PhD[1]

Purpose: To report the effectiveness, disease-specific outcomes, and safety of cultivated oral mucosal epithelial sheet transplantation (COMET), with the primary objective of visual improvement.

Design: Noncomparative, retrospective, interventional case series.

Participants: This study involved 46 eyes in 40 patients with complete limbal stem cell deficiency (LSCD) who underwent COMET for visual improvement. These LSCD disorders fell into the following 4 categories: Stevens-Johnson syndrome (SJS; 21 eyes), ocular cicatricial pemphigoid (OCP; 10 eyes), thermal or chemical injury (7 eyes), or other diseases (8 eyes).

Methods: Best-corrected visual acuity (BCVA) and ocular surface grading score were examined before surgery; at the 4th, 12th, and 24th postoperative week; and at the last follow-up. Data on COMET-related adverse events and postoperative management were collected. The outcomes in each disease category were evaluated separately.

Main Outcome Measures: The primary outcome was the change in median logarithm of the minimum angle of resolution (logMAR) BCVA at the 24th postoperative week. The secondary outcome was the ocular surface grading score.

Results: Median logMAR BCVA at baseline was 2.40 (range, 1.10 to 3.00). In SJS, logMAR BCVA improved significantly during the 24 weeks after surgery. In contrast, the BCVA in OCP was improved significantly only at the 4th postoperative week. In 6 of the 7 thermal or chemical injury cases, logMAR BCVA improved after planned penetrating keratoplasty or deep lamellar keratoplasty. Grading scores of ocular surface abnormalities improved in all categories. Of 31 patients with vision loss (logMAR BCVA, >2) at baseline, COMET produced improvement (logMAR BCVA, ≤2) in 15 patients (48%). Visual improvement was maintained with long-term follow-up (median, 28.7 months). Multivariate stepwise logistic regression analysis showed that corneal neovascularization and symblepharon were correlated significantly with logMAR BCVA improvement at the 24th postoperative week ($P = 0.0023$ and $P = 0.0173$, respectively). Although postoperative persistent epithelial defects and slight to moderate corneal infection occurred in the eyes of 16 and 2 patients, respectively, all were treated successfully with no eye perforation.

Conclusions: Long-term visual improvement was achievable in cases of complete LSCD. Cultivated oral mucosal epithelial sheet transplantation offered substantial visual improvement even for patients with end-stage severe ocular surface disorders accompanying severe tear deficiency. Patients with corneal blindness such as SJS benefited from critical improvement of visual acuity.

Financial Disclosure(s): The author(s) have no proprietary or commercial interest in anymaterials discussed in this article. *Ophthalmology 2013;120:193–200 © 2013 by the American Academy of Ophthalmology.*

Corneal renewal and repair are mediated by corneal epithelial stem cells situated mainly in the limbus, the narrow region between the cornea and the bulbar conjunctiva.[1] Damage or depletion of the corneal epithelial stem cells, known as limbal stem cell deficiency (LSCD), leads to conjunctival invasion that results in vascularization and scarring of the cornea with an associated profound loss of vision.[1] Limbal stem cell deficiency can be caused by Stevens-Johnson syndrome (SJS), ocular cicatricial pemphigoid (OCP), and thermal or chemical injury, which are all characterized by the loss of corneal epithelial stem cells. Such LSCD may cause severe ocular surface diseases (OSDs) in which cicatrization resulting from conjunctival fibrosis, symblepharon, and severe dry eye greatly disrupt visual function and can progress gradually with chronic inflammation.[2–4] To date, few effective medical or surgical treatments for severe OSDs have been available.[5–15]

Since 1998, the authors have used amniotic membrane transplantation to treat severe OSDs. Amniotic membrane exhibits an anti-inflammatory effect and also acts as a substrate for epithelialization.[16] The results of previous studies have shown that amniotic membrane transplantation alone[17,18] or amniotic membrane transplantation combined with limbal transplantation[6,19,20] promoted epithelialization, reduced pain, reconstructed the fornix, and minimized inflammation of the ocular surface to a remarkable degree in

ISSN 0161-6420/13/$–see front matter
http://dx.doi.org/10.1016/j.ophtha.2012.07.053